

# Practical Local Geoid Modelling of Benin City, Nigeria from Gravimetric Observations Using the Modified Stokes Integral

Oduyebo, O. F. \*; Ono M. N. and Eteje, S. O.

Department of Surveying and Geoinformatics, Nnamdi Azikiwe University, Awka, Nigeria

\*Corresponding Author: [jimioduyebo@yahoo.com](mailto:jimioduyebo@yahoo.com)

**Abstract**— The geometric heights obtained from GNSS observations cannot be used for engineering works as they are not reduced to the geoid. This study presents practical local geoid modelling from gravimetric observations using the modified Stokes integral for engineering applications in Benin City. A total of 52 points were observed with GNSS receivers and a gravimeter to respectively obtain their positions and absolute gravity values. The theoretical gravity values of the points were computed on the Clarke 1880 ellipsoid to obtain their local gravity anomalies. The modified Stokes integral was applied to compute the geoid heights of the points. The combined topographic effect was applied to the computed geoid heights of the points to obtain their precise geoid heights. The mean of the precise geoid heights of the points was computed to obtain the local gravimetric geoid model of the study area. The determined geoid model was validated for its reliability as well as the accuracy using the RMSE index. It is recommended that the use of assumed, as well as handheld GPS receiver heights for engineering works should be totally abolished as this study has established the local geoid model of Benin City.

**Keywords**— gravimetric observations, integration, local geoid, modelling, modified Stokes integral.

## I. INTRODUCTION

The geoid is an equipotential (level) surface of the earth's gravity field which coincides with mean sea level (MSL) in the open oceans. As such, the geoid provides a meaningful reference frame for defining heights. The importance of accurately modelling the geoid has increased in recent years with the advent of satellite positioning systems such as the Global Navigation Satellite System (GNSS). GNSS provides height information relative to a best-fitting earth ellipsoid rather than the geoid (Seager *et al.*, 1999; Yilmaz and Arslan, 2006). To convert ellipsoidal heights derived from GNSS to conventional (and meaningful) orthometric heights, the relationship between the geoid and the ellipsoid must be

known (Kotsakis and Sideris, 1999; Yilmaz and Arslan, 2006). The fundamental relationship that ties ellipsoidal heights obtained from Global Navigation Satellite System (GNSS) measurements and heights with respect to a vertical datum established using spirit levelling and gravity data, is to the first approximation given by (Heiskanen and Moritz, 1967; Krynski and Lyszkowicz, 2006; Oluyori *et al.*, 2018) as:

$$h = H + N \quad (1)$$

Where  $h$  is the ellipsoidal height,  $H$  is the orthometric height, and  $N$  is the geoid undulation. Figure 1 shows the relationship between the orthometric, geoid and ellipsoidal heights.

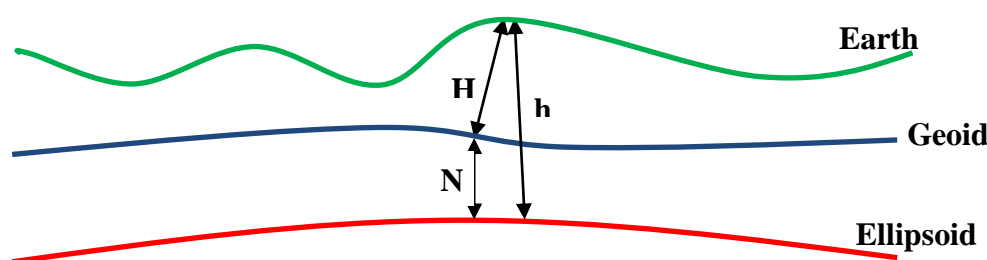


Fig. 1: Relationship between Orthometric, Geoid and Ellipsoidal Heights

Source: Eteje *et al.* (2018)



**1.2 Integration of Stokes's Formula**

According to Eteje *et al.* (2018), using the modified Stokes integral given in equation (2), the geoid heights of points can be computed if their gravity anomalies and

$$N = \frac{r\Delta g}{8\gamma} \left( \begin{array}{l} -6\sin^2 \psi_o \ln \left\{ \sin \left( \frac{\psi_o}{2} \right) + \sin^2 \left( \frac{\psi_o}{2} \right) \right\} + 16\sin \left( \frac{\psi_o}{2} \right) + 12\sin^2 \left( \frac{\psi_o}{2} \right) \\ -24\sin^3 \left( \frac{\psi_o}{2} \right) - 12\sin^4 \left( \frac{\psi_o}{2} \right) - 4\cos \psi_o + 5\cos 2\psi_o - 1 \end{array} \right) \quad (3)$$

Where *N* is the geoidal height of individual point,  $\psi_o$  is the surface spherical radius,  $\gamma$  is the theoretical as well as normal gravity,  $\Delta g$  is the gravity anomaly and  $r = R$  is the mean radius of the earth. So, the computation of the geoid heights of points using equation (3) requires the use of the surface spherical radius,  $\psi_o$ , theoretical, as well as normal gravity values,  $\gamma$ , gravity anomalies,  $\Delta g$ , and the mean radius of the earth,  $r = R$  of the points.

**1.3 Surface Spherical Radius Computation**

The surface spherical radius,  $\psi_o$  is computed as (Shrivastava *et al.*, 2015)

$$\cos \psi = \sin \varphi \sin \varphi^1 + \cos \varphi \cos \varphi^1 \cos (\lambda^1 - \lambda) \quad (4)$$

Where,

$$g_{T\text{Clarke1880}(B)} = 9.78051938 \left( \begin{array}{l} 1 + 0.005247466 \sin^2 \varphi \\ -0.0000087985 \sin^2 2\varphi \end{array} \right) \text{ms}^{-2} \quad (5)$$

Where,

$g_{T\text{Clarke1880}}$  = Theoretical gravity on the Clarke 1880 ellipsoid  
 $\varphi$  = Station latitude

**1.4 Gravity Anomaly Computation**

The gravity anomaly,  $\Delta g$ , is the difference between the observed gravity value (*g*) reduced to the geoid, and a normal, or theoretical, computed gravity value ( $\gamma_o$ ) at the mean earth ellipsoid, where, the actual gravity potential on the geoid equal the normal gravity potential at the ellipsoid, at the projection of the same terrain point on the geoid and the ellipsoid respectively, that is (Dawod, 1998 and Eteje *et al.*, 2019)

$$\Delta g = g - \gamma_o \quad (6)$$

Considering the nature of the topography of the earth surface, which is irregular in shape, there are two basic types of gravity anomalies (free air and Bouguer anomalies). In this study, it was only the free air correction that was applied.

geographic coordinates are known. Featherstone and Olliver (1997) gave the integration of equation (2), as well as the Stokes integral as

- $\varphi$  = Mean latitude of the points
- $\varphi^1$  = Latitude of individual point
- $\lambda$  = Mean longitude of the points
- $\lambda^1$  = Longitude of individual point

**1.5 Theoretical Gravity Computation**

To obtain the local gravity anomalies of points in a study area, the normal, as well as the latitude gravity, is computed on a specified ellipsoid. That is, the ellipsoid adopted for geodetic computation in the area or region of study. Eteje *et al.* (2018) gave the model for the computation of the theoretical gravity on the Clarke 1880 ellipsoid as

**1.6 Free Air Correction**

This is the first step for reducing topography effects. It simply corrects for the change in the elevation of the gravity meter, considering only air (hence a free-air) being between the meter and selected datum. According to Aziz *et al.* (2010), this correction is added to the observed gravity because the increased radial distance of the station from the centre of the Earth results in a lower observed gravity value than if the station were at the local datum. The formula to calculate the magnitude of the reduction in practice is given by Eteje *et al.* (2019) as

$$g_{FA} = -\frac{2g}{r} H_s = -308.6 H \mu Gal \quad (7)$$

$$= -0.3086 H m Gal$$

Where,

- H* = Station orthometric height in metres
- g* = Mean value of gravity (980500 mGal)
- r* = Mean radius of the Earth

**1.7 Mean Radius of the Earth Computation**

The mean radius of the earth,  $r = R$  was computed using:

$$R = \sqrt{MN} \quad (8)$$

Where  $M$  is the radius of curvature along the meridian section and  $N$  is the radius of curvature in prime vertical. The formula for computation of the radius of curvature in prime vertical,  $N$  is given as (Ono, 2009)

$$N = \frac{a}{(1 - (2f - f^2) \sin^2 \varphi)^{3/2}} = \quad (9)$$

while that for computation of the radius of curvature in meridian section,  $M$  is given as (Kotsakis, 2008)

$$M = \frac{a(1 - e^2)}{(1 - e^2 \sin^2 \varphi)^{3/2}} \quad (10)$$

Where,

$a$  = Semi-major axis

$\varphi$  = Latitude of an observation point

$e^2 = 2f - f^2$  = Eccentricity squared (Eteje *et al.*, 2019)

$f = \frac{a - b}{a}$  = Flattening

$b$  = Semi-minor axis

### 1.8 Combined Topographic Effect Computation

To obtain a precise geoid height of a point, the combined topographic effect is calculated and applied to the computed geoid height of the point. The formula for the computation of the combined topographic effect,

$\delta N_{Comb}^{Topo}$  is given as (Sjöberg, 2000 and Kuczynska-Siehien *et al.*, 2016):

$$\delta N_{Comb}^{Topo} = -\frac{2\pi G \rho}{\gamma} \left[ H^2 + \frac{2}{3R} H^2 \right] \quad (11)$$

Where  $G$  is the earth gravitational constant,  $\rho$  is density,  $R$  is the mean radius of the earth and  $H$  is the orthometric height of observation point which can be obtained from the DTM of the area.

### 1.9 The Geoid Model

The final gravimetric geoid model is the mean of the geoid heights computed with equations (3) and (11) and it is obtained using

$$\text{Gravimetric Geoid Model} = \frac{1}{n} \sum_{i=1}^n N_i \quad (12)$$

Where,

$N_i$  = Geoid height of points computed using equations (3) and (11),

$n$  = Total number of points

### 1.10 Accuracy of the Gravimetric Geoid Model

The accuracy of the determined local gravimetric geoid model is obtained using the Root Mean Square Error, RMSE index. To evaluate the determined local gravimetric geoid model accuracy, the orthometric heights computed from the differences between the model geoid heights and ellipsoidal heights of some selected points are compared with their (the points) respective orthometric heights obtained from spirit levelling to get the residuals. The computed residuals and the total number of points are used to calculate the RMSE of the model. The Root Mean Square Error, RMSE index for the computation of gravimetric geoid model accuracy as given by Kao *et al.* (2017) and Eteje and Oduyebo (2018) is

$$RMSE = \pm \sqrt{\frac{V^T V}{n}} \quad (13)$$

Where,

$V = H_{Observed} - H_{Model}$  (Residual)

$H_{Observed}$  = Observed Orthometric Height of Point

$H_{Model}$  = Model Orthometric Height of Point

$n$  = Number of Points

## II. METHODOLOGY

The adopted methodology was divided into different stages of data acquisition, data processing, and results presentation and analysis. Figure 3 shows the adopted methodology flow chart.

### 2.1 Data Acquisition

A total of 52 points were used in the study. The points included two primary control stations (XSU 92 and XSU 100 were respectively located in Edo College and School of Nursing premises). The other 50 points were selected along the major roads of the City (See Figure 4). Spirit levelling was carried out on 3 of the 50 points for validation purpose. GNSS observations were carried out using CHC 900 dual-frequency GNSS receivers to obtain the coordinates and ellipsoidal heights of the points. The observations were carried out relative to control station XSU 92 using the static method (See Figures 5 and 6).



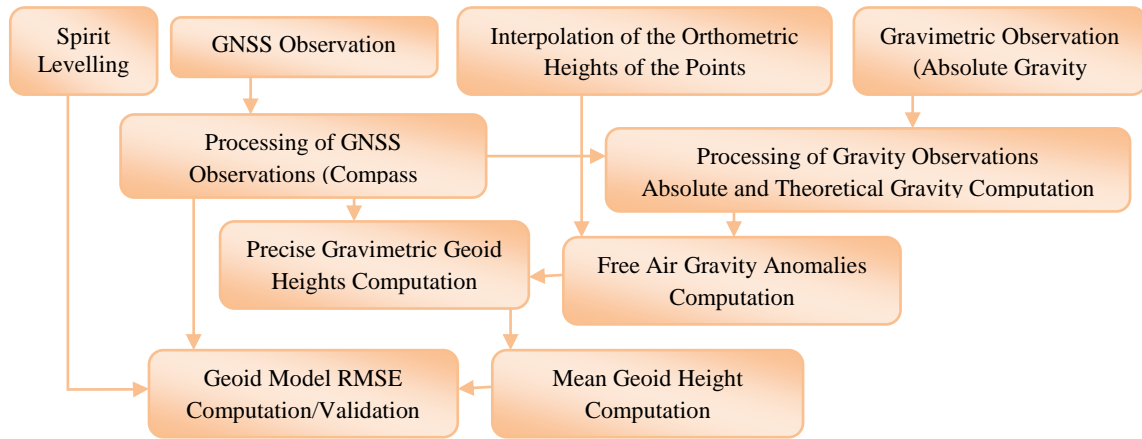


Fig 3: Flow Chart of the Adopted Methodology

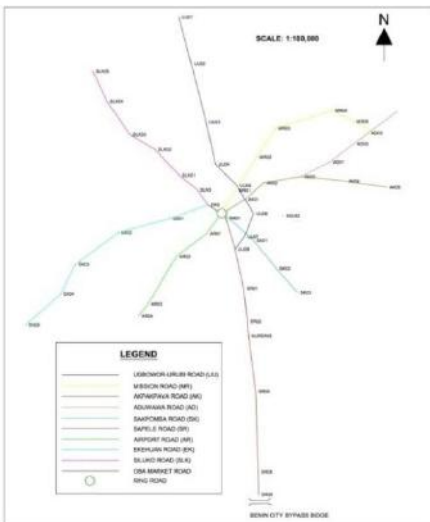


Fig 4: Selected GPS and Gravity Points



Fig. 5: Base Receiver at Control Station XSU92



Fig. 6: Rover Receiver at One of the Selected Points (RR01) at Ring Road

The selected points were observed with a gravimeter (SCINTREX CG-5 Autograv Gravimeter) to obtain their absolute gravity values. The observations were carried by an expert, a Geophysicist from Mountain Top University, Ibafo, Ogun State. The gravity observations of the points

were carried out in seven different loops relative to a point whose absolute gravity value was known and located within the Benin City Airport premises (See Figures 7 and 8).



Fig. 7: Gravimeter Set over Reference Station at Benin City Airport



Fig. 8: Gravimeter at One of the Selected Points at Bypass along Benin-Sapele Road

Spirit levelling was carried out on the 3 validation points, as well as test points using control station XSU100 as a

point of known orthometric height to obtain their practical heights. The levelling of the test points was carried out in

two loops. The first loop started from control station XSU100 to TP1 and closed back on control station XSU100 while the second loop levelling started from TP1

through TP2 to TP3 and closed back on TP1. Figure 9 shows the validation points' levelling loops.

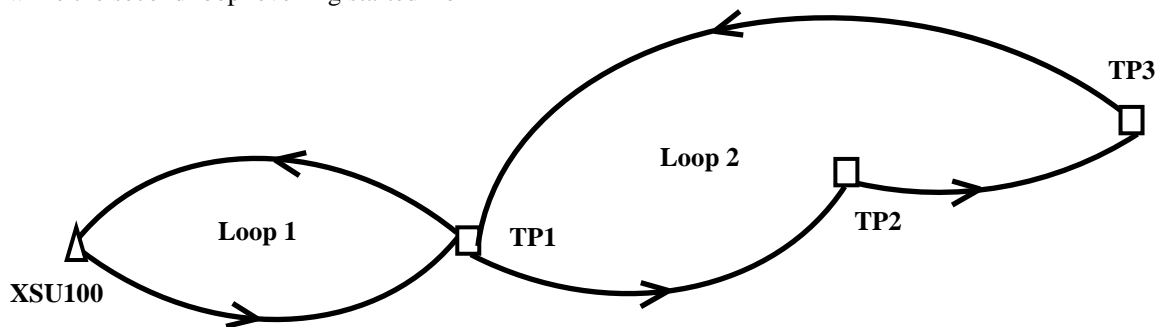


Fig. 9: Validation Points Levelling Loops

## 2.2 Data Processing

The GNSS observations were respectively downloaded and processed with HcLoader and Compass Post-processing software to obtain the positions and the ellipsoidal heights of the points. The coordinates and the ellipsoidal heights of the points were processed in Minna datum. The gravity observations of the points were processed by the expert who carried out the observation to obtain their absolute gravity values. All the necessary corrections such as drift correction, etc were applied during the processing. The theoretical gravity values of the points were computed on the local (Minna) datum ellipsoid (Clarke 1880 ellipsoid) using the latitude coordinates of the points, as well as equation (5). The gravity anomalies of the points were computed by finding the differences between the absolute gravity values of the points and their corresponding theoretical gravity values, as well as using equation (6). The computation of the free air correction requires the application of the orthometric heights of the points. And these were obtained by interpolation using the orthometric heights and the absolute gravity values of the two primary control stations (XSU 100 and XSU 96). The orthometric heights of the points were interpolated as there was no Digital Terrain Model (DTM) of the study area. The free air correction was applied to the computed gravity anomalies of the points using equation (7). The free air and the Bouguer gravity anomalies of the points were computed but the free air gravity anomalies were used in the study. This is because the geoid heights of the two primary control stations obtained from their known orthometric and ellipsoidal heights approximated the geoid heights of the stations computed using the free air gravity anomalies, as well as equation (3). The gravimetric geoid heights of the points were computed with the geographic coordinates, free air gravity anomalies and the theoretical

gravity of the points using equation (3). The computation of the gravimetric geoid heights of the points required the application of the spherical radius and the mean radius of the earth. The spherical radius and the mean radius of the earth were respectively computed using equations (4) and (8). Also, the computation of the mean radius of the earth required the computation of the radius of curvature in prime vertical and in meridian section using equations (9) and (10) respectively. The computed gravimetric geoid heights of the points using equation (3) were co-geoid heights. To obtain precise gravimetric geoid heights of the points, the combined topographic effect has to be computed and applied to the co-geoid heights. The combined topographic effect was computed using equation (11). The final local gravimetric geoid model of the study area was obtained by finding the mean of the precise geoid heights of the points using equation (12). The spirit levelling of the validation points was reduced using the height of instrument method, as well as collimation method. The RMSE, as well as the accuracy of the model, was computed by finding the square root of the mean of the differences between the model and the observed orthometric heights of the validation points and the two control stations using equations (13).

## III. RESULTS PRESENTATION AND ANALYSIS

### 3.1 Analysis of the GNSS Observation Results

The DGPS observations were carried out to obtain the coordinates and ellipsoidal heights of the selected points. The DGPS observations were processed using Compass post-processing software. From the processing of the DGPS observations results, it was seen that the processed observations passed both the Network Adjustment Test and the X-Square (Chi-square) Test. This implied that the normal matrix generated was a regular one and inverted accordingly for the calculation of residuals.

### 3.2 Analysis of the Validation Points Levelling

Table 1 presents the closure errors/accuracy of the two loops of the validation points levelling. The levelling of the validation points was done to obtain the orthometric heights of the validation points. The levelling was carried in two loops. The first loop started from XSU100 to TP1 and closed back on XSU100 while the second loop started from TP1 through TP2 to TP3 and closed back on TP1.

From Table 1 it is seen that the closure error of the first loop is -0.006m while the second loop closure error is 0.009m which were within millimetres standard. The results were accepted as the closing errors of the two loops. The high accuracy of the levelling was as a result of the fairly flat topography of the study area, the observer's know-how and the equipment used.

Table 1: Known and Observed Heights of the Closing Stations

Station	Description	H <sub>(known)</sub> (m)	H <sub>(observed)</sub> (m)	ΔH (m)
Loop 1	Starting and Closing Station (XSU100)	76.377	76.383	-0.006
Loop 2	Starting and Closing Station (TP1)	60.912	60.903	0.009

### 3.3

#### Analysis of the Gravimetric Geoid Model

Table 2 and Figures 10a and 10b respectively present the coordinates of the selected points, their corresponding computed local gravimetric geoid heights and the determined geoid model, and their surface and contour plots. The gravimetric geoid heights of the points were computed using the integration of modified Stokes' integral. The gravity anomalies of the points used for the computation of the local gravimetric geoid heights of the points were computed on the Clarke 1880 ellipsoid which is the ellipsoid adopted for local geodetic computation in

Nigeri

a. From Table 2, it is seen that the determined geoid model (mean of geoid heights) is 2.066m. This implied that to convert ellipsoidal heights of points to orthometric heights in Benin City, 2.066m will be subtracted from the ellipsoidal heights of the points. Also, from Figures 10a and 10b, it is seen that at the centre, there are depressions with small cliffs closed to them while at some distances from the centre there are small depressions which implies that the geoid heights of the study area vary with no constant value.

Table 2: Coordinates of the Selected Points and their Respective Local Gravimetric Heights

STATION	Northing	Easting	Free Air Geoid Height, N Corrected for Combined Topographic Effect
XSU92	257998.9800	357763.3720	2.086
RR01	257885.3227	355124.0166	2.420
SR01	254586.4919	355927.3773	1.588
SR02	253034.8393	356093.6672	1.978
SR04	249754.3940	356486.6091	2.520
SR05	245976.7564	356615.1406	2.802
SR06	244918.0916	356628.3396	3.266
XSU100	252357.6855	356143.1412	2.098
AR01	257163.2838	354191.2450	0.685
AR02	256084.6701	352774.2792	0.720
AR03	253855.5374	351456.5724	1.436
AR04	253286.3364	351007.1375	1.439
UU01	267318.6942	352896.8470	4.658
UU02	265145.3515	353468.5482	3.498
UU03	262403.8368	354173.5295	1.981
UU04	260409.1199	354602.6925	1.276
UU05	259407.1043	355613.0973	1.346
UU06	258099.7270	356379.9681	1.489
UU07	257012.1709	355964.2081	1.329
UU08	256422.9868	355521.4167	1.263
AD01	260514.8753	359958.1194	2.986

AD02	261374.7703	361092.6917	4.019
AD03	261867.2294	361745.9231	4.420
AK01	258765.7701	355982.5939	1.376
AK02	259528.7811	356853.3277	1.473
AK03	259836.4068	358613.7581	2.252
AK04	259620.2060	360694.5908	3.101
AK05	259332.1257	362604.6963	3.954
MR01	259195.6591	355569.5117	1.300
MR02	260751.5081	356528.1658	1.488
MR03	262096.1924	357412.2545	1.614
MR04	262930.8267	360077.3193	4.037
MR05	262428.2213	361076.8116	4.313
SK01	256829.9481	356396.3673	1.500
SK02	255516.1557	357459.1723	2.035
SK03	254396.4836	358439.3812	2.379
EKS	258508.0691	354257.9420	0.665
SLK0	259220.8416	353748.2583	0.668
SLK01	259894.0672	352909.3470	0.781
SLK02	261105.4062	351776.4441	1.326
SLK03	261813.3387	350594.2641	1.736
SLK04	263367.4251	349531.4676	2.688
SLK05	264774.9356	348869.1903	3.357
EK01	257862.9575	352479.5790	0.078
EK02	257209.3523	350068.7731	0.983
EK03	255709.4653	348058.3750	1.729
EK04	254327.4139	347366.3299	2.001
EK05	252877.2407	345740.0760	2.516
AIRPORT	256224.9627	352774.5959	0.578
<b>GEOID MODEL (MEAN OF GEOID HEIGHTS) =</b>			<b>2.066m</b>

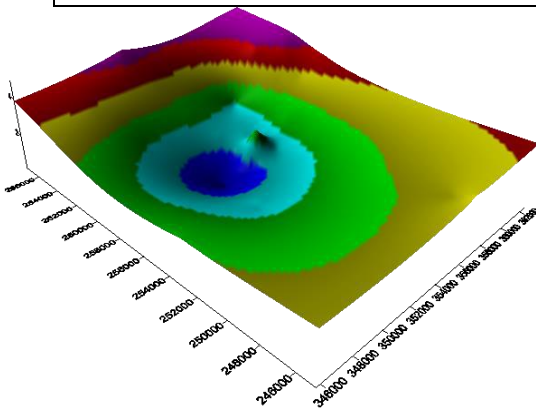


Fig 10a: Surface Plot of Gravimetric Geoid Heights of the Selected Points

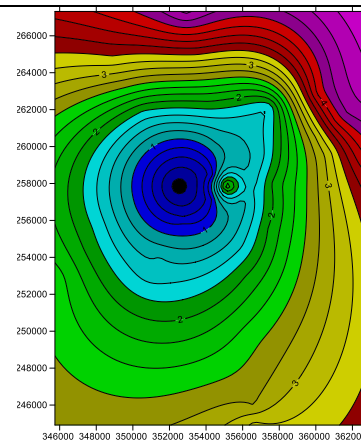


Fig 10b: Contour Plot of Gravimetric Geoid Heights of the Selected Points

### 3.4 Analysis of the Accuracy/Validation of the Determined Geoid Model

Table 3 and Figure 11 respectively present the computed RMSE of the geoid model and the plot of the model and the observed orthometric heights. This was



done to present the consistency, as well as the reliability of the determined geoid model. It can be seen from Table 3 that the computed RMSE, as well as the accuracy of the determined gravimetric geoid model, is 0.412m. This implies that ellipsoidal heights can be converted to orthometric height with an accuracy of 41cm using the

determined geoid model. It can also be seen from Figure 11 that the model and the observed orthometric heights of the validation points/stations are identical in shape which also implies the high reliability, as well as consistency of the determined gravimetric geoid model.

Table 3: Observed and Model Orthometric Height, and Model RMSE/Accuracy

STATION	DGPS ELLIPSOIDAL HEIGHT (m)	GEOID MODEL (m)	MODEL ORTHOMETRIC HEIGHT (m)	OBSERVED ORTHOMETRIC HEIGHT (m)	DIFF. B/W MODEL & KNOWN ORTHOMETRIC HEIGHTS (m)	DIFF. SQUARE D
XSU92	106.668	2.066	104.602	105.441	0.839	0.704
XSU100	78.399	2.066	76.333	76.377	0.044	0.002
TP1	63.122	2.066	61.056	60.912	-0.144	0.021
TP2	53.326	2.066	51.260	51.605	0.345	0.119
TP3	64.069	2.066	62.003	62.068	0.065	0.004
<b>RMSE =</b>						<b>0.412m</b>

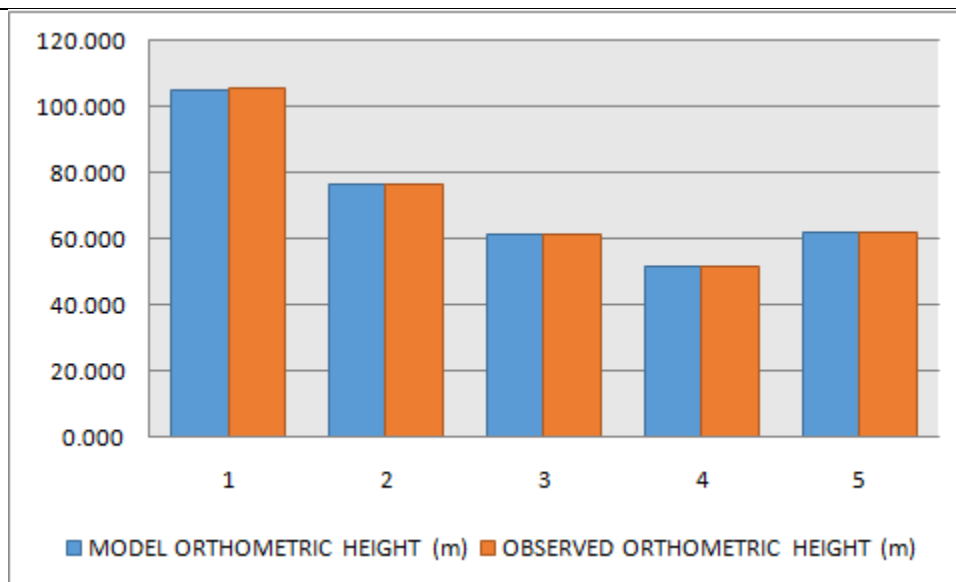


Fig. 11: Validation Points Model and Observed Orthometric Heights

**IV. CONCLUSIONS AND RECOMMENDATIONS**

1. The local geoid model of Benin City has been determined to be 2.066m using the gravimetric method of integration of modified Stokes formula.
2. The study has shown that ellipsoidal heights can be converted to orthometric heights with an accuracy of 0.412m using the determined geoid model.
3. It is recommended that the determined geoid model should be applied whenever ellipsoidal heights are to be converted to practical, as well as orthometric heights in Benin City.
4. It is also recommended that the use of assumed, as well as handheld GPS receiver heights should be

totally abolished as this study has established the local geoid model of Benin City.

**REFERENCES**

- [1] Aziz, N., Majid, B. and Jörg, E. (2010). Gravity and Magnetic Data Acquisition Over a Segment of the Møre-Trøndelag Fault Complex. *NGU Report 2010.049*.
- [2] Dawod, D. M. (1998). A National Gravity Standardization Network for Egypt. Published Ph.D Dissertation of the Department of Surveying Engineering, Shoubra Faculty of Engineering, Zagazig University. [https://www.academia.edu/794554/The\\_egyptian\\_national\\_gravity\\_standardization\\_network\\_ENGSN97\\_](https://www.academia.edu/794554/The_egyptian_national_gravity_standardization_network_ENGSN97_). Accessed 20th September 2019.

- [3] Eteje, S. O. (2015). Determination of the Local Geoid Model Using the Geometric (GPS/Levelling) Method for Evboriaria in Benin City, Edo State. Unpublished MSc Thesis of the Department of Surveying and Geoinformatics, Nnamdi Azikiwe University, Awka.
- [4] Eteje, S. O. and Oduyebo, F. O. (2018): Local Geometric Geoid Models Parameters and Accuracy Determination Using Least Squares Technique. *International Journal of Innovative Research and Development (IJIRD)*, Vol. 7, No 7, pp 251-257. DOI: 10.24940/ijird/2018/v7/i7/JUL18098.
- [5] Eteje, S. O., Oduyebo, O. F. and Olulade, S. A. (2018). Procedure for the Determination of Local Gravimetric-Geometric Geoid Model. *International Journal of Advances in Scientific Research and Engineering*, Vol. 4, No. 8, pp 206-214. DOI: 10.31695/IJASRE.2018.32858.
- [6] Eteje, S. O., Oduyebo, O. F. and Oluyori, P. D. (2019). Modelling Local Gravity Anomalies from Processed Observed Gravity Measurements for Geodetic Applications. *International Journal of Scientific Research in Science and Technology*, Vol. 6, No. 5, pp 144-162. DOI: 10.32628/IJSRST196515.
- [7] Eteje, S. O., Oduyebo, O. F. and Oluyori, P. D. (2019). Procedure for Coordinates Conversion between NTM and UTM Systems in Minna Datum Using AllTrans and Columbus Software. *International Journal of Scientific Research in Science and Technology*, Vol. 6, No. 5, pp 128-143. DOI: 10.32628/IJSRST196517.
- [8] Eteje, S. O., Oduyebo, O. F. and Ono, M. N. (2019). Derivation of Theoretical Gravity Model on the Clarke 1880 Ellipsoid for Practical Local Geoid Model Determination. *Scientific Research Journal (SCIRJ)*, Vol. 7, No 2, pp 12-19. DOI: 10.31364/SCIRJ/v7.i2.2019.P0219612.
- [9] Eteje, S. O., Ono, M. N. and Oduyebo, O. F. (2018). Practical Local Geoid Model Determination for Mean Sea Level Heights of Surveys and Stable Building Projects. *IOSR Journal of Environmental Science, Toxicology and Food Technology (IOSR-JESTFT)*, Vol. 12, No. 6, pp 30-37.
- [10] Featherstone, W. E. and Olliver, J. G. (1997). A Method to Validate Gravimetric-Geoid Computation Software Based on Stokes's Integral Formula. *Journal of Geodesy*, Vol. 71, pp 571-576.
- [11] Helsenkanen, W. A. and Moritz, H. (1967): Physical Geodesy. Freeman and Company, San Francisco, Geoid Modelling and Height Determination for Engineering Applications. [www.abu.edu.ng/publications/2009-07-11-122210\\_2930.pdf](http://www.abu.edu.ng/publications/2009-07-11-122210_2930.pdf). Accessed January 26, 2018.
- [12] Kao, S., Ning, F., Chen, C. and Chen, C. (2017): Using Particle Swarm Optimization to Establish a Local Geometric Geoid Model. *Boletim de Ciências Geodésicas*, Vol. 23, No. 2, pp. 327-337.
- [13] Kotsakis, C. (2008): Transforming Ellipsoidal Heights and geoid Undulations between Different Geodetic Reference Frames. *Journal of Geodesy*, Vol. 82, No. 4, Pp 249-260.
- [14] Kotsakis, C., Sideris, M. G. (1999): On the Adjustment of Combined GPS/Levelling/ Geoid Networks. *Journal of Geoid* Vol. 73, pp 412-421.
- [15] Krynski J. And Lyszkowicz, A. (2006): Fitting gravimetric Quasigeoid Model to GPS/Levelling Data in Poland. First International Symposium of the International Gravity Field Service, Istanbul, Turkey.
- [16] Kuczynska-Siehnien, J., Lyszkowicz, A. and Birylo, M. (2016). Geoid Determination for the Area of Poland by the Least Squares Modification of Stokes' Formula. *Acta Geodyn. Geomater*, Vol. 13, No. 1, Pp 19-26.
- [17] Oluyori, P. D., Ono, M. N. and Eteje, S. O. (2018). Comparison of Two Polynomial Geoid Models of GNSS/Levelling Geoid Development for Orthometric Heights in FCT, Abuja. *International Journal of Engineering Research and Advanced Technology (IJERAT)*, Vol. 4, No. 10, pp 1-9. DOI: 10.31695/IJERAT.2018.3330.
- [18] Oluyori, P. D., Ono, M. N. and Eteje, S. O. (2018). Computations of Geoid Undulation from Comparison of GNSS/Levelling with EGM 2008 for Geodetic Applications. *International Journal of Scientific and Research Publications*, Vol. 8, No. 10, pp 235-241. DOI: 10.29322/IJSRP.8.10.2018.p8230.
- [19] Ono, M. N. (2009): On Problems of Coordinates, Coordinate Systems and Transformation Parameters in Local Map Production, Updates and Revisions in Nigeria. FIG Working Week, Eilat, Israel.
- [20] Seager, J., Collier, P., and Kirby, J. (1999): Modelling Geoid Undulations with an Artificial Neural Network. *IEEE*, International Joint Conference, Volume 5, pp 3332 - 3335.
- [21] Shrivastava, P., Sahoo, L. and Stalin, M. (2015). Geoid Models for Indian Territory. *IJSRSET*, Vol. 1 No. 4, Pp 180-187.
- [22] Sjöberg, L. E. (2000). On the Topographic Effects by the Stokes Helmert Method of Geoid and Quasi-Geoid Determinations. *Journal of Geodesy*, Vol. 74 No. 2, Pp 255-268. DOI: 10.1007/s001900050284 in Kuczynska-Siehnien, J., Lyszkowicz, A. and Birylo, M. (2016). Geoid Determination for the Area of Poland by the Least Squares Modification of Stokes' Formula. *Acta Geodyn. Geomater*, Vol. 13, No. 1, Pp 19-26.
- [23] Yilmaz, M. and Arslan, E. (2006): Application of Fuzzy Logic Theory to Geoid Height Determination. First International Symposium of the International Gravity Field Service, Istanbul, Turkey.